

Cite this: *Dalton Trans.*, 2013, **42**, 8815

Crystal structure and magnetic properties of $\text{Cr}_3\text{Te}_5\text{O}_{13}\text{Cl}_3$ †

Iwan Zimmermann,^a Reinhard K. Kremer,^b Patrick Reuvekamp^b and Mats Johnsson^{*a}

A new chromium tellurite oxochloride, $\text{Cr}_3\text{Te}_5\text{O}_{13}\text{Cl}_3$, has been prepared by solid-state reaction and the crystal structure was determined by single crystal X-ray diffraction. The compound crystallizes in the non-centrosymmetric space group $P2_12_12_1$ with the unit cell $a = 4.90180(10)$ Å, $b = 17.3394(2)$ Å, $c = 17.5405(2)$ Å, $Z = 4$, $R_1 = 0.0282$. The Cr^{3+} ions have octahedral $[\text{CrO}_6]$ oxygen coordination, the Te^{4+} ions have one sided $[\text{TeO}_3]$ and $[\text{TeO}_3\text{Cl}]$ coordinations. The $[\text{CrO}_6]$ octahedra are edge sharing and form chains extending along [100]. These are connected by corner sharing $[\text{TeO}_3]$ and $[\text{TeO}_3\text{Cl}]$ groups to form layers parallel to (110). The layers are connected by weak interactions in between Te^{4+} in the layers and Cl^- ions located in between. The compound undergoes antiferromagnetic ordering at ~ 34 K with a Weiss constant of -230 K. Isothermal magnetization measurements reveal a critical field of about 0.25 T above which the magnetization *versus* field changes from linear to a Brillouin-like saturation behaviour. The frustration ratio amounts to ~ 6.8 indicative of sizable competing antiferromagnetic spin-exchange interaction. The dielectric constant ϵ (6 kHz) amounts to ~ 7.9 and decreases by about 1% on cooling from 50 K to liquid helium temperatures.

Received 14th March 2013,
Accepted 9th April 2013

DOI: 10.1039/c3dt50706h

www.rsc.org/dalton

Introduction

Oxohalide compounds comprising p-block lone-pair elements such as Se^{4+} , Te^{4+} , or Sb^{3+} often exhibit unusual structural and physical properties because both the stereochemically active lone-pair and the halide ion contribute to open up the crystal structures by terminating structural elements and by occupying space in the nonbonding regions. The nonbonding side of the lone-pair elements naturally faces other lone-pair elements or halide ions to generate extended nonbonding volumes. This may lead to formation of (i) layered compounds with only weak van der Waals interactions in between the layers, as found in *e.g.* $\text{Sb}_3\text{TeO}_6\text{Cl}$,¹ $\text{Pb}_3\text{Te}_2\text{O}_6\text{Cl}_2$,² $\text{CuSbTeO}_3\text{Cl}_2$,³ $\text{Bi}_3\text{Te}_4\text{O}_{10}\text{Cl}_5$,⁴ $\text{ZnSbO}_3\text{Cl}_2$ ⁵ or (ii) compounds having a 3D

network with channels where the lone-pairs or the halide ions reside *e.g.* $\text{Ni}_{15}\text{Te}_{12}\text{O}_{34}\text{Cl}_{10}$ ⁶ and $\text{Co}_5(\text{SeO}_3)_4\text{X}_2$ ($\text{X} = \text{Cl}, \text{Br}$).⁷ The asymmetric bonding character of the lone-pair cation has been utilized in synthesis strategies to search for new low-dimensional compounds with unusual magnetic properties as for example spin-frustration^{8,9} or for non-centrosymmetric compounds showing non-linear optical properties.^{10–12}

The majority of compounds containing Cr^{3+} are oxides and CrOCl is the only oxo-chloride previously reported, plus some hydrates; *e.g.* $\text{Cs}_2\text{CrCl}_5(\text{H}_2\text{O})_4$ and $\text{K}_2\text{CrCl}_5(\text{H}_2\text{O})$.^{13–16} Only one tellurite containing Cr^{3+} is previously described in the literature; $\text{Cr}_2\text{Te}_4\text{O}_{11}$.¹⁷ To the best of our knowledge the present compound $\text{Cr}_3\text{Te}_5\text{O}_{13}\text{Cl}_3$ is the first chromium oxo-chloride comprising a p-element lone pair cation.

Experimental

The new compound $\text{Cr}_3\text{Te}_5\text{O}_{13}\text{Cl}_3$ was synthesized *via* chemical reactions in sealed evacuated silica tubes. Needle shaped single crystals were obtained from a mixture of TeO_2 (Sigma-Aldrich 99+%), Cr_2O_3 (Sigma-Aldrich) and CrCl_3 (Sigma Aldrich) in the molar ratio 3 : 1 : 1. The reaction was carried out in a muffle furnace at 500 °C for 1 month. The product was a mixture of green crystals of the title compound and unreacted starting material. Single crystals of the title compound did grow on top of the powder so it was easy to separate them.

^aDepartment of Materials and Environmental Chemistry, Stockholm University, SE-106 91 Stockholm, Sweden. E-mail: iwan.zimmermann@mmk.su.se, mats.johnsson@mmk.su.se; Fax: +46 8 152187; Tel: +46 8 162169

^bMax Planck Institute for Solid State Research, Heisenbergstrasse 1, D-70569 Stuttgart, Germany. E-mail: rekre@fkf.mpg.de, p.reuvekamp@fkf.mpg.de; Fax: +49 711 689 1689; Tel: +49 711 689 1688

†Electronic supplementary information (ESI) available: Tables of atomic coordinates and equivalent isotropic displacement parameters, bonding distances and angles, and Bond Valence Sum (BVS) calculations. Further details on the crystal structural investigations can be obtained from the Fachinformationszentrum Karlsruhe, Abt. PROKA, 76344 Eggenstein-Leopoldshafen, Germany (fax +49-7247-808-666; E-mail: crysdata@fiz-karlsruhe.de) on quoting the depository number CSD 425829. See DOI: 10.1039/c3dt50706h



Single crystal X-ray diffraction experiments were carried out on an Oxford Diffraction Xcalibur3 diffractometer equipped with a graphite monochromator. The data collection was carried out at 293 K using MoK α radiation, $\lambda = 0.71073$ Å. Data reduction was done with the software CrysAlis RED that was also employed for the analytical absorption correction.¹⁸ The structure solution was carried out with SHELXS and the refinement with SHELXL¹⁹ in the WINGX²⁰ environment. Restraints were applied to oxygen O5 and O13 to refine their anisotropic temperature parameters to positive-definite values. Atomic coordinates and isotropic temperature parameters for all atoms are given in the ESI.[†] Structure data are reported in Table 1. Structure plots are made with the program DIAMOND.²¹

For the magnetic measurements crystals were separated manually and ground in an agate mortar before putting in a gelatine capsule. The magnetic susceptibilities of a powder compact of Cr₃Te₅O₁₃Cl₃ have been measured under field-cooling and zero field-cooling conditions with a PPMS Physical Property Measurement System and an MPMS Magnetic Property Measurement System (both Quantum Design) at temperatures between 1.8 and 300 K in magnetic fields up to 7 Tesla. The heat capacity of a small powder sample (≈ 1.5 mg) was measured with a PPMS system equipped with a ³He cryostat employing the relaxation method.

Table 1 Crystal data and structure refinement parameters for Cr₃Te₅O₁₃Cl₃

Empirical formula	Cr ₃ Te ₅ O ₁₃ Cl ₃
Formula weight (g mol ⁻¹)	1108.35
Temperature (K)	293
Wavelength (Å)	0.71073
Crystal system	Orthorhombic
Space group	P2 ₁ 2 ₁ 2 ₁
<i>a</i> (Å)	4.90180(10)
<i>b</i> (Å)	17.3394(2)
<i>c</i> (Å)	17.5405(2)
α (°)	90
β (°)	90
γ (°)	90
Volume (Å ³)	1490.84(4)
<i>Z</i>	4
Density _{calc.} (g cm ⁻³)	4.938
Absorption coefficient (mm ⁻¹)	12.341
<i>F</i> (000)	1948
Crystal color	Green
Crystal habit	Needle
Crystal size (mm ³)	0.071 \times 0.0149 \times 0.0129
Theta range for data collection (°)	4.2–32.32
Index ranges	$-7 \leq h \leq 7$ $-24 \leq k \leq 25$ $-25 \leq l \leq 17$
Reflections collected/unique	21 195/4956 ($R_{\text{int}} = 0.0474$)
Independent reflections	4416
Data/restraints/parameters	4956/12/217
Goodness-of-fit on <i>F</i> ²	0.992
Final <i>R</i> indices ^a	$R_1 = 0.0282$
$[I > 2\sigma(I)]$	$wR_2 = 0.0504$
<i>R</i> indices (all data)	$R_1 = 0.0346$ $wR_2 = 0.0517$
Flack parameter	0.01(3)
Largest diff. peak and hole (e Å ⁻³)	1.462 and -2.032

$$^a R_1 = \sum ||F_0| - |F_c|| / \sum |F_0|; wR_2 = \{\sum [w(F_0^2 - F_c^2)]^2 / \sum [w(F_0^2)]^2\}^{1/2}.$$

The temperature dependence of the dielectric susceptibility was measured with an Andeen-Hagerling, Inc. AH 2700 ultra-precision capacitance bridge on an *in situ* pressed pellet of 3 mm diameter and a thickness of ~ 0.5 mm and in external magnetic fields up to 3 Tesla.

Results and discussion

Crystal structure

The new tellurium oxo-halide compound Cr₃Te₅O₁₃Cl₃ crystallizes in the non-centrosymmetric orthorhombic space group P2₁2₁2₁. The crystal structure can be regarded as layered with the layers parallel to (110) and only weak Te–Cl interactions connect the layers, see Fig. 1.

There are three crystallographically different chromium atoms all exhibiting distorted octahedral coordination. The Cr atoms only coordinate O atoms as a consequence of their relatively high Lewis acid strength. The Cr–O distances range from 1.915(4) Å to 2.021(4) Å. The chromium octahedra are edge sharing and form chains along [100], see Fig. 2. The chromium chains are surrounded by the tellurium polyhedra to build up layers in the (110) plane, see Fig. 1.

All five crystallographically different Te atoms are coordinated to oxygen forming [TeO₃] trigonal pyramids with distances in the range 1.812(4)–2.154(4) Å. Te3 has also a bonding distance to Cl1 that is 2.5630(16) Å so that a [Te3O₇Cl] see-saw coordination is formed. The Te1 and Te5 polyhedra are isolated, whereas the polyhedra around Te2, Te3 and Te4 polymerise *via* corner sharing to form a [Te₃O₇Cl] group. There are also several long Te–O and Te–Cl distances that are at the verge of being included in the primary bonding sphere. Brown suggests as a working definition that ligands that contribute

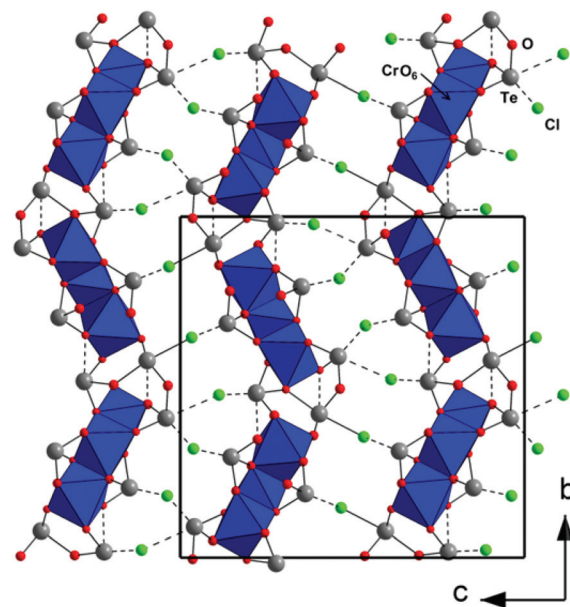


Fig. 1 Crystal structure of Cr₃Te₅O₁₃Cl₃ shown along [100]. The layers stack along [001] and are held together by weak Te–Cl interactions.

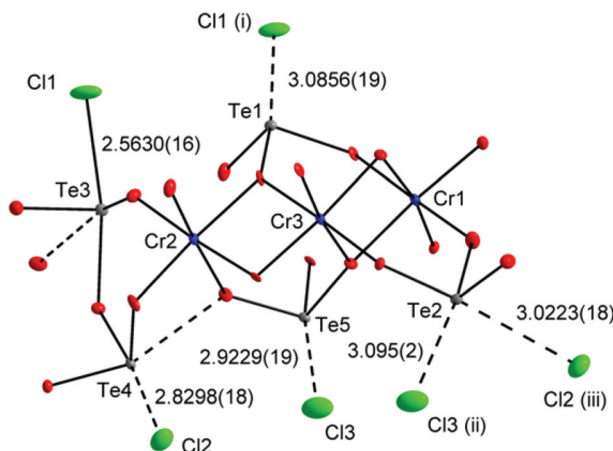


Fig. 2 Asymmetric unit with selected symmetry equivalents. Long Te–O and Te–Cl interactions are indicated by dashed lines. The $[\text{CrO}_6]$ octahedra form chains along [100] via edge sharing.

with at least 4% of the valence of the cation shall be considered as coordinated²² and this implies Te–O distances <2.66 Å and Te–Cl distances <3.05 Å, see Fig. 2. Including all such Te–O and Te–Cl distances will result in the following coordination polyhedra: $[\text{Te}_1\text{O}_3]$, $[\text{Te}_2\text{O}_3\text{Cl}]$, $[\text{Te}_3\text{O}_4\text{Cl}]$, $[\text{Te}_4\text{O}_4\text{Cl}]$, and $[\text{Te}_5\text{O}_3\text{Cl}]$. If all these O and Cl atoms at the verge of the primary coordination sphere are considered as bonded then only the $[\text{Te}_1\text{O}_3]$ polyhedra will be isolated and the other will constitute a $[\text{Te}_{17}\text{O}_{42}\text{Cl}_{12}]$ polymer chain that extends along [001]. The Cl₂ and Cl₃ atoms thus act mainly as counter ions as indicated by their low bond valence sum values (0.46 and 0.36 respectively) and they hold together the layered structure by weak interactions with tellurium atoms of neighbouring layers; this interaction is not symmetric and the chlorine atom is always closer to one of the tellurium atoms it interacts with, see Fig. 1.

Magnetic, thermal and dielectric properties

The magnetic susceptibilities reveal an antiferromagnetic phase transition at ~ 34 K evidenced by a sharp spike which is very sensitive to the magnitude of the external magnetic field. Above 0.3 T the spike is smeared out and a broad anomaly reminiscent of ferromagnetic order remains, see Fig. 3. Isothermal magnetization measurement also reveals a critical field of about 0.25 T above which the magnetization *versus* field changes from linear to a Brillouin-like saturation behaviour, see Fig. 4. The high-temperature inverse susceptibilities follow Curie–Weiss behaviour (eqn (1))

$$\chi_{\text{mol}} = \frac{C}{T - \Theta_{\text{CW}}} X \quad (1)$$

with a Curie constant C corresponding to an effective magnetic moment of $3.9\mu_{\text{B}}$ per Cr³⁺ ion, in good agreement with an $S = 3/2$ spin-only effective moment typically expected for Cr³⁺ ions in an octahedral environment. The Curie–Weiss temperature, Θ_{CW} , is fitted to -230 K indicating predominant antiferromagnetic spin-exchange interaction. The frustration ratio (eqn (2))

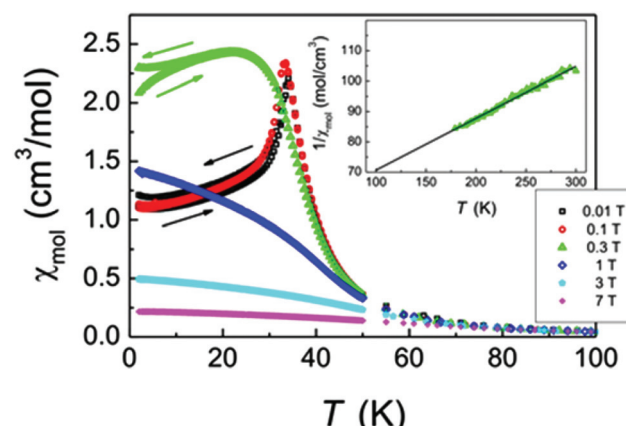


Fig. 3 Magnetic susceptibility of $\text{Cr}_3\text{Te}_5\text{O}_{13}\text{Cl}_3$ measured at different magnetic fields. The antiferromagnetic ordering at 34 K is suppressed by magnetic fields above ~ 0.3 T. The inset displays the inverse susceptibility measured in a field of 0.3 T. The slope of the straight solid line corresponds to an effective magnetic moment of $3.9\mu_{\text{B}}$ per Cr³⁺ ion. The straight line intersects the temperature axis at about -230 K indicating predominantly an antiferromagnetic spin-exchange interaction.

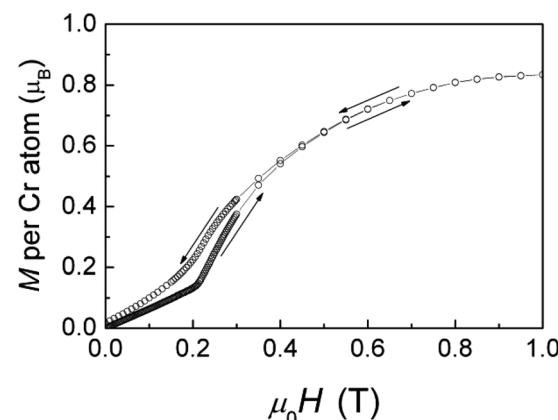


Fig. 4 Isothermal magnetization data of $\text{Cr}_3\text{Te}_5\text{O}_{13}\text{Cl}_3$ collected at 2 K.

amounts to ~ 6.8 indicative of sizable competing antiferromagnetic spin-exchange interaction

$$f = -\Theta_{\text{CW}}/T_{\text{C}} \quad (2)$$

The heat capacity reveals a sluggish weak magnetic anomaly consistent with long-range antiferromagnetic ordering at 34 K, see Fig. 5. The entropy contained in the magnetic anomaly by integration of the quantity C_p/T is found to be ~ 1 J mol⁻¹ K⁻¹, which corresponds to only $\sim 10\%$ of Rln4, expected for an $S = 3/2$ system; the remaining 90% apparently must have been already removed in antiferromagnetic short-range ordering processes above T_{C} consistent with the presence of one-dimensional character of the chains of edge sharing $[\text{CrO}_6]$ octahedra along [100] supporting low-dimensional magnetic behaviour.

Magnetoelectric coupling may be expected to be very small since Cr³⁺ with its 3d³ electronic configuration, in a first approximation constitutes a spin-only system with small

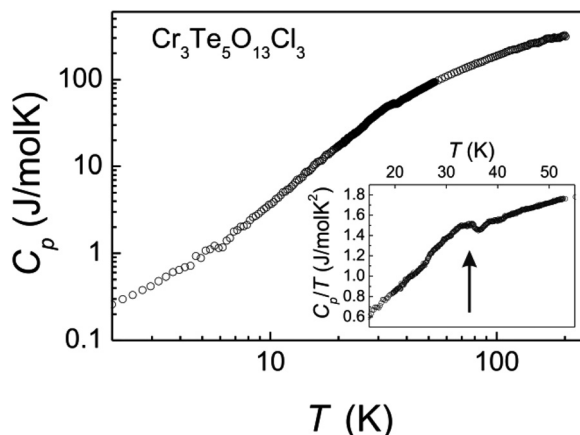


Fig. 5 Temperature dependence of the heat capacity, $C_p(T)$, for $\text{Cr}_3\text{Te}_5\text{O}_{13}\text{Cl}_3$. The inset displays the quantity C_p/T emphasizing the magnetic phase transition near 34 K (arrow).

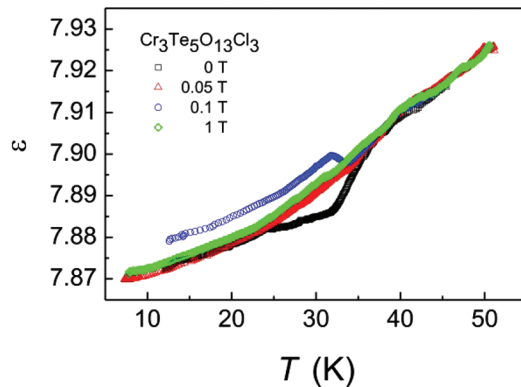


Fig. 6 Temperature dependence of the dielectric constant, ϵ , of a polycrystalline sample of $\text{Cr}_3\text{Te}_5\text{O}_{13}\text{Cl}_3$.

orbital contributions to its magnetic moment and hence small coupling to lattice degrees of freedom. Nevertheless, magnetic ordering below 34 K induces an anomaly in the dielectric properties. Fig. 6 displays the temperature dependence of the dielectric constant of a polycrystalline sample of $\text{Cr}_3\text{Te}_5\text{O}_{13}\text{Cl}_3$. ϵ (6 kHz) amounts to ~ 7.9 and decreases by about 1% on cooling from 50 K to liquid helium temperatures. Below 34 K $\epsilon(T)$ exhibits a magnetoelectric anomaly which is very sensitive to small external magnetic fields. In zero external field $\epsilon(T)$ shows a drop which is washed out by a field of 0.05 T. At 0.1 T the anomaly is inverted and $\epsilon(T)$ exhibits an increase and a ridge below 34 K. In fields above 1 T the magnetoelectric anomaly is completely smeared out.

Conclusions

The new tellurium oxo chloride $\text{Cr}_3\text{Te}_5\text{O}_{13}\text{Cl}_3$ was synthesized via chemical reactions in evacuated and sealed silica tubes. The compound crystallizes in the non-centrosymmetric space group $P2_12_12_1$. The crystal structure is built from layers

stacking parallel to the (110) plane, which are held together by weak Te-Cl interactions. The chromium atoms form CrO_6 octahedra, which are arranged in chains *via* edge sharing along [110]. The tellurium atoms form $[\text{TeO}_3]$ trigonal pyramids because of the stereochemically active lone pair. Magnetic measurements show an antiferromagnetic ordering at ~ 34 K. The transition is shown to be very sensitive to the strength of the magnetic field applied. Above a critical field of ~ 0.3 T the magnetization *versus* field changes from linear to a Brillouin-like saturation behaviour. The dielectric constant ϵ (6 kHz) amounts to ~ 7.9 and decreases by about 1% on cooling from 50 K to liquid helium temperatures. Below 34 K $\epsilon(T)$ exhibits a magnetoelectric anomaly which is very sensitive to small external magnetic fields.

Acknowledgements

This work has in part been carried out through financial support from the Swedish Research Council.

Notes and references

- 1 J. A. Alonso, E. Gutiérrez-Puebla, A. Jerez, A. Monge and C. Ruiz-Valero, *J. Chem. Soc., Dalton Trans.*, 1985, 1633.
- 2 Y. Porter and P. S. Halasyamani, *Inorg. Chem.*, 2003, **42**, 205.
- 3 R. Becker, M. Johnsson, R. K. Kremer and P. Lemmens, *Solid State Chem.*, 2003, **5**, 1411.
- 4 M. K. Kim, V. Jo, D. W. Lee and K. M. Ok, *Dalton Trans.*, 2010, **39**, 6037.
- 5 V. Jo, M. K. Kim, D. W. Lee, I. W. Shim and K. M. Ok, *Inorg. Chem.*, 2010, **49**, 2990.
- 6 D. Zhang, M. Johnsson, S. Lidin and R. K. Kremer, *Dalton Trans.*, 2013, **43**, 1394.
- 7 R. Becker, M. Prester, H. Berger, P. H. Lin, M. Johnsson, D. Drobac and I. Zivkovic, *J. Solid State Chem.*, 2007, **180**, 1051.
- 8 M. Johnsson, K. W. Törnroos, F. Mila and P. Millet, *Chem. Mater.*, 2000, **12**, 2853.
- 9 R. Becker, M. Johnsson, R. K. Kremer, H.-H. Klaus and P. Lemmens, *J. Am. Chem. Soc.*, 2006, **128**, 15469.
- 10 C.-F. Sun, C.-L. Hu, X. Xu, B.-P. Yang and J.-G. Mao, *J. Am. Chem. Soc.*, 2011, **133**, 5561.
- 11 C.-F. Sun, C.-L. Hu and J.-G. Mao, *Chem. Commun.*, 2012, **48**, 4220.
- 12 S. D. Nguyen and P. S. Halasyamani, *Inorg. Chem.*, 2013, **52**, 2637.
- 13 H.-E. Forsberg, *Acta Chem. Scand.*, 1962, **16**, 777.
- 14 J. Angelkort, A. Wölfel, A. Schönleber, S. van Smaalen and R. K. Kremer, *Phys. Rev. B: Condens. Matter*, 2006, **80**, 144416.
- 15 S. C. Nyburg, B. Soptrajanov, V. Stefov and V. M. Petrushevski, *Inorg. Chem.*, 1997, **36**, 2248.



16 B. M. Casari, A. K. Eriksson and V. Langer, *Z. Anorg. Allg. Chem.*, 2006, **632**, 101.

17 P. G. Meunier, B. Frit and J. Galy, *Acta Crystallogr., Sect. B: Struct. Crystallogr. Cryst. Chem.*, 1976, **32**, 175.

18 Oxford diffraction, *CrysAlisCCD* and *CrysAlisRED*, Oxford Diffraction Ltd., Abingdon, Oxfordshire, England, 2006.

19 G. M. Sheldrick, *Acta Crystallogr., Sect. A: Fundam. Crystallogr.*, 2008, **64**, 112.

20 L. J. Farrugia, *J. Appl. Crystallogr.*, 1999, **32**, 837.

21 G. Bergerhoff, *DIAMOND*, Bonn, Germany, 1996.

22 I. D. Brown, *The Chemical Bond in Inorganic Chemistry: The Bond Valence Model*, Oxford University Press, New York, 2002.

